COMPUTER GRAPHICS AND IMAGE PROCESSING (1974) 3, (163–177)

SURVEY

Unsharp Masking and Related Image Enhancement Techniques

LEO LEVI
Jerusalem College of Technology, P.O. Box 16031, Jerusalem, Israel

Communicated by T. S. Huang

Received May 1, 1973

Unsharp masking—in many forms—is a frequent technique in image enhancement. Various versions of unsharp masking are described together with the related dynamic exposure control techniques. Detailed analyses of these techniques are appended.

1. INTRODUCTION

Image restoration consists of the reduction of degradations caused by the original imaging process. The degradations generally include a distortion of the spatial frequency spectrum so that image restoration requires a modification of the spectrum of the degraded image. Such modification may be performed directly in the Fourier transform plane of the image by means of spatial filtering or by means of convolving the image with a spread function which is the Fourier transform of the desired filter function.

Frequently, the original imaging process had a transfer function (tf) which decreases from the origin, and the restoration technique must therefore employ a tf which rises from the origin. Such a tf may be implemented in the Fourier plane by using a spatial filter with transmittance rising away from the origin. Alternatively, it may be implemented by convolving the degraded image with a spread function which is the Fourier transform of the desired filter function. Now, note that a tf rising above its origin value implies a spread function which is negative over a finite region.[1] Since spread functions of simple devices are usually nonnegative, the desired spread function

[1] Since the tf is the Fourier transform of the spread function, $[T(\nu) > T(o)]$ implies

$$|\int P(\mathbf{x}) e^{i2\pi \nu \cdot x}\, d\mathbf{x}| > |\int P(\mathbf{x})\, d\mathbf{x}|.$$

The triangle inequality shows that this is impossible on the assumption of $P(\mathbf{x})$ real and positive everywhere:

$$|\int P(\mathbf{x}) e^{i2\pi \nu \cdot x}\, dx| \leqslant \int |P(\mathbf{x}) e^{i2\pi \nu \cdot x}|\, d\mathbf{x} = \int P(\mathbf{x}) |e^{i2\pi \nu \cdot x}|\, d\mathbf{x}.$$
$$\equiv \int P(\mathbf{x})\, d\mathbf{x} = |\int P(\mathbf{x})\, d\mathbf{x}|.$$

Clearly, the first member can not exceed the last member. Hence the initial condition implies that $P(\mathbf{x})$ is *not* real and positive everywhere.

is occasionally implemented by means of a compound spread function consisting of a positive and a negative component individually implemented. Such techniques are called "unsharp masking" by analogy with the photographic prototype of the method.

When the total areas under the positive and negative components of the spread function are equal, any uniform area will be rendered at zero level, regardless of its absolute level, be it white, black, or anything between these. Deviations from zero level will occur only in regions of changing object signal level. Such arrangements may be called *balanced masking*.

A number of such techniques, and the related dynamic exposure control technique, are here described. Since these techniques are often nonlinear, their analyses are complicated. They are presented in the Appendix.

2. UNSHARP MASKING

2.1 *Photographic Unsharp Masking*

In photographic unsharp masking, two versions of the photographic image are printed in register. One of these is a sharp negative and the other a blurred positive. The combination corresponds to a spread function consisting of a sharp positive peak surrounded by a broad, shallow negative zone. This corresponds to a tf which first rises and drops only at higher spatial frequencies and which, therefore, compensates somewhat for the degradation of intermediate frequencies present in the original photograph. Although this method is useful in photography in general [1,2], it was first applied in roentgenology [3] and later in aerial photography [4] and map making [5].

In general, such printing will lower the modulation everywhere in the image—except to the extent that the photographic process compensates for this by means of a high gamma. It has been suggested that the phenomenon of spurious resolution—which implies a negative value of tf—will produce regions where the subtraction will yield absolute enhancement of modulation [6].

Because of the nonlinearity of the photographic process—and especially because of the essential nonlinearity of the mask production—photographic unsharp masking is a nonlinear process not representable, in general, in terms of a tf.

The expression describing the unsharp masking process is derived in the Appendix. With the proper choice of gammas (γ), the final image signal may be written as

$$s_f = a\, s_n(\bar{}_n{}^{\gamma} \circledast P_m), \tag{1}$$

where a is a proportionality factor, $s_n = s_0 \bigcirc P_0$ is the signal of the degraded image, s_0 is the original object signal and P_0, P_m are the point spread functions of the original photographing system and the mask-making process, respectively.

The essential nonlinearity introduced by the negative exponent γ prevents

us from finding a simple expression for the spectrum. We may, however, write a linear approximation to the unsharp masking process. This would be valid for objects exhibiting only small modulation values. As shown in the Appendix, this approximation yields a final image spectrum of the form

$$S_f = aS_0T_0(1 - bT_m), \tag{2}$$

where S_0 is the original object spectrum, T_0, T_m are the tf's of the original photographing system and the mask-making process, respectively, and b is a constant involving the gammas and relative mean transmittances in the various photographic stages.

Thus, with linear approximation, the tf of photographic unsharp masking is

$$T_f = a(1 - bT_m). \tag{3}$$

This implies that a drop in T_0 at high frequencies could be compensated for (up to frequency ν_0) by choosing T_m and b such that $[T_0(\nu)T_f(\nu)]$ equals unity, i.e.,

$$bT_m(\nu) = 1 - [aT_0(\nu)]^{-1} \tag{4}$$

for all $\nu < \nu_0$.

If the positive and negative transparencies were individually prepared from the same master, with imaging tf's T_p and T_n and gammas γ_p and γ_n, respectively, the following masking tf would result [7]:

$$T_f = \gamma_p T_p - \gamma_n T_n. \tag{5}$$

A balanced version of unsharp photographic masking, combined with printing on a very high gamma photographic emulsion, can be used to print continuous-tone objects with a line-drawing quality. This has been called the tone-line process [7,8].

The operation of this process can be understood as allowing only rapid modulation changes to cause significant deviations, both positive and negative, from a mean exposure in the image. When exposed onto a high-gamma emulsion so that the mean exposure is below the operating range of the emulsion, only the positive exposure spikes will appear in the final image.

Photographic masking, with both positive and negative equally sharp, but slightly out of register, is called "relief," if it is balanced, and "pseudo-relief," if slightly unbalanced [7].

2.2 *Phosphor Quenching and Herschel-Effect Photography*

The unsharp masking process requires the subtraction of a blurred image from a sharp one. Instead of doing this by means of a blurred "negative" transparency, as described in Section 2.1, it may be accomplished by means of quenching effects. *Quenching* refers to the process where radiation, because of its particular spectral character, reduces the image modulation generated by radiation of a different wavelength. It is observed both in luminescence and photography.

Specifically, some photoluminescent phosphors, which are excitable by

ultraviolet radiation, exhibit a pronounced luminance reduction when irradiated at a longer wavelength [9]. A similar effect is observed in photography. When photographic emulsions are exposed, at sufficiently high levels, to radiation to which they are sensitive, grains in the emulsion become developable—a *latent image* is formed. In some emulsions this state of developability is drastically reduced—the latent image is partly erased—upon subsequent irradiation at wavelengths beyond the range of sensitivity. This reduction in effective exposure due to longer wavelength radiation is called Herschel effect [10] and can be used for unsharp masking purposes [11,12].

One "unsharp masking" technique, using a quenchable phosphor, is named "fluoro-dodge" and is illustrated in Fig. 1. The negative is contact printed onto the emulsion; but, instead of illuminating the negative uniformly, it is illuminated by means of a blurred positive image formed on the phosphor screen. This phosphor-screen image is the result of two forms of illumination: uniform illumination with exciting ultraviolet radiation and the quenching action of the blurred infrared image formed on the phosphor screen at the same time. The exposure at any point on the emulsion is proportional to the product of two factors: the transmittance of the negative and the luminance of the phosphor-screen image at that point. Since the phosphor luminance at every point is reduced according to a blurred rendition of the negative, unsharp masking results [13].

Fluoro-dodge can be used in a balanced process, so that only regions of changing density will appear in the final image. When this is combined with high-contrast photographic printing, outlining is obtained [14].

The analysis of fluoro-dodge processing is presented in the Appendix. Assuming the quenching process to be linear, the processed image will have a modulation distribution given by

$$s_f = a\, s_n\, [1 - b\, s_n \circledast P_m], \tag{6}$$

where the symbols were defined following Eq. (1).

If the image modulation is small, the linear approximation becomes valid

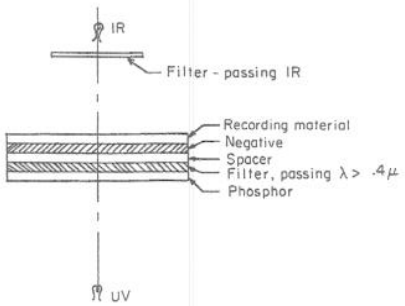

FIG. 1. Fluoro-dodge technique. The phosphor is uniformly excited by radiation from the uv source and selectively quenched by radiation for the ir source. The negative casts a blurred ir shadow on the phosphor, controlling the quenching. The phosphor luminance contact-prints the negative onto the emulsion. Blurring is controlled by the spacer.

and takes, again, the form of Eq. (2); it has the same form as that for photographic unsharp masking.

The same method could be applied using the Herschel effect for "quenching" the photographic emulsion directly. Alternatively, the two exposures—one in focus and one, at longer wavelengths, out of focus—could be made sequentially [11]. A third method, which has been used successfully, employs the technique of shaped apertures to yield similarly shaped spread functions.

With this method, both exposures can be made simultaneously: We simply place a shaped filter, passing only longer wavelengths, into the aperture to cover the zones which are to be negative in the resulting spread function [12].

A very elegant, and far simpler, method has been used. When a lens suffering from chromatic aberration images a point source and is properly focused for the short wavelengths, the image of a point will consist of a sharp image of short-wavelength light and a blurred image of long-wavelength light. If the lens has the proper amount of chromatic aberration, this blurred image can be used for unsharp masking in conjunction with photographic material exhibiting a significant Herschel effect [12]. This technique can, of course, be used in a scanning device also.

Assuming the Herschel effect itself to be linear, the unsharp masking process is described by

$$s_p(x) = a\,[s_n^{-\gamma} - b\,s_n \circledast P_m]. \tag{7}$$

See the Appendix.

The linearized version again has the form of Eq. (2).

2.3 *Dual Spot Scanning*

The above unsharp masking techniques all involved simultaneous formation of all the image elements. Now we describe a sequential technique where the image is built up, element by element, by means of scanning.

Although multiple spot scanning is possible, we discuss here only the dual spot system. There the two spots are shaped to correspond, respectively, to the positive and negative portions of the desired spread function. The transmitted light from each of these spots is received on its individual photodetector and the outputs of the two photodetectors are subtracted (subsequent to possible amplification). In less sophisticated implementations of this technique, the positive spot diameter is made small compared to the desired resolution performance and the negative spot considerably larger, with no effort at controlling the distribution within each spot. This technique, too, is closely related to "unsharp masking" and is often referred to as such.

For each spot the photodetector–unit output, i.e., the product of the spot flux and the photodetector–unit sensitivity and gain, at maximum object transmittance, may be termed the "weight" of that spot channel. When the weights of the positive and negative spots are equal, the system is said to be

balanced. The output of a balanced system will vanish whenever the object region being scanned is uniformly transmitting; indeed, the output will vanish in any region where the transmittance *gradient* is constant. In practice, with such a system, only regions of rapidly changing transmittance will yield a significant output signal.

This form of "unsharp masking" is most readily treated in terms of transfer function theory: the tf of the system is simply the difference between the tf's of the two scanning spots (i.e., the Fourier transforms of their spread functions). The weight of each of the two-spot channels must be applied to their respective tf's to establish their relative magnitudes before finding their difference. In terms of this theory, a balanced system has a tf which vanishes at the origin, so that very low spatial frequencies are eliminated.

The dual-spot technique has been implemented in various forms. Usually, two different spectral regions are used to permit separating the two channels. The spots may be generated as the images of two shaped apertures, covered by different spectral filters [15]. They may be generated on two different cathode-ray tubes and then combined optically for scanning; after scanning they may be separated again by means of a dichroic beam splitter [16], or they may be provided with mutually orthogonal polarization to facilitate their subsequent separation [17,18]. A particularly elegant approach employs a white scanning spot which is imaged by an optical system suffering from severe chromatic aberration. The spot is focused for the short wavelengths. This will result in a sharp blue image, surrounded by a reddish halo. Again, a dichroic beamsplitter splits the light from the sharp central spot from that of the blurred red image [19].

3. DYNAMIC EXPOSURE CONTROL

Dynamic exposure control is an entirely different approach to image enhancement. However, it is in many ways equivalent to unsharp masking. Here, image segments, containing many resolution elements, are exposed sequentially, with exposure controlled by the object transmittance[2] averaged over the segment. This is accomplished by imaging the object transparency in the plane of the photodetectors (such as photographic film) and scanning this transparency with a large luminous spot. The exposure rate at any one instant is then controlled according to the total flux transmitted at that instant. This control may be made either open- or closed-loop. In the open-loop technique, we may expect a linear relationship between the rate of exposure and the quantity of transmitted flux. In the closed-loop technique, an effort is made to control the exposure rate in a manner such that the average exposure rate remains constant. This is done by sensing the difference between the actual exposure rate and a reference rate, and using this difference to adjust the exposure rate to reduce this difference.

[2] It should be noted that these techniques can be used with luminous objects. With such objects, the scanning "spots" are apertures as imaged on the object. More often, this technique is used with passive opaque or transparent objects which are scanned by the image of a luminous spot. For simplicity of terminology, the following discussion is worded for transparent objects; the modifications necessary to apply to the other types of object are obvious.

In this section we present one illustration each of open- and closed-loop techniques.

3.1. Velocity Dynamic Exposure Control

As just stated, in dynamic exposure control, the controlled quantity is the rate of exposure. Since exposure is the product of irradiance and time, this rate can be controlled either by controlling the irradiance or the scanning velocity. Control of velocity is particularly suitable to an open-loop technique and it has been used in that application [21].

In a practical system, a small fraction of the transmitted light flux is deflected, measured, and the scanning velocity made proportional to this flux. Since the effective exposure time of any one element is inversely proportional to the scanning velocity, the total instantaneous exposure remains constant with the relative exposure of individual resolution elements still proportional to the transmittance of the object transparency.

The technique is illustrated in Fig. 2. A spot on the face of the cathode ray tube traces out a raster on the tube face, thereby scanning the transparency, T. Lens L_1 images this transparency on the recording medium, R. A small fraction of the transmitted light is deflected by mirror M, which may be a plane piece of glass and collected on a phototube P by lens L_2. The detected irradiance level controls the raster scanning velocity, as generated by the deflection unit D.

If the spot is made quite large compared to the image element regions, the effect will be to equalize the mean exposure over the various image regions. This tends to reduce the overall density range considerably. This is true because often the largest density variations occur in going from one image region to another, for instance, in going from a bright object image element in a sunny region (image region) to a dark object in a shadow region. When sunny and shadow regions are equalized, the density range is reduced and may, consequently, fit into the transfer characteristic of the recording medium.

If the spot is comparable in size to the image element regions, the effect will be primarily one of edge enhancement: regions of constant transmittance gradient will all be exposed to the reference level and only regions of changing gradient will appear darker or lighter than this.

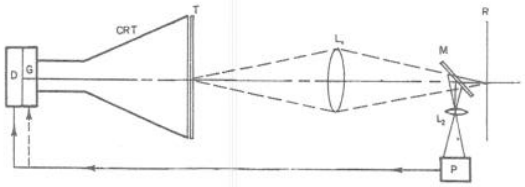

FIG. 2. Dynamic exposure control. A large spot on the face of the cathode-ray tube scans the object transparency, which is imaged on the recording medium R by lens L. At any instant, a fixed fraction of the total transmitted light is concentrated on the photodetector, P, after deflection by mirror, M. The output of the photodetector controls the deflection rate, D, in velocity control, and the electron-gun grid, G, in luminance control.

The quantitative analysis of this device is given in the Appendix. In brief, the velocity is proportional to the correlation integral of the spot point spread function (P) and the object transmittances (τ); the exposure is, therefore, inversely proportional to this. It is given by

$$c\tau\,[P \circledast (P \odot \tau)^{-1}], \tag{8}$$

where c is a constant.

This is a nonlinear expression and therefore does not lend itself to statement in terms of a tf. When application is restricted to low-amplitude signals, this is shown, in the Appendix, to lead to the following expression for the tf of the process:

$$T_p = c\,[1 - |T_s|^2], \tag{9}$$

where T_s is the Fourier transform of P—the "tf" of the scanning spot. If T_s is negligible, except at low spatial frequencies, this process can be seen to reduce the overall tf at these low frequencies, compensating for the degradations at the higher frequencies in the original imaging system which produced the object being processed.

3.2 *Closed-Loop Dynamic Exposure Control (Log Etron)*

In the closed-loop approach to dynamic exposure control, the illumination is controlled so that the total transmitted light tends to be constant. The method is illustrated in the block diagram, Fig. 3. Light from a cathode-ray tube (or any other modulatable light source) scans the "object" transparency. The transmitted light exposes the recording medium and its area integral is measured by a photosensor. This measurement is compared to a reference signal and the difference between the two is amplified. The amplified signal then controls the spot brightness [22].

The optical portion of the system, enclosed in the broken outline, is identical to that of the velocity-controlled dynamic exposure control system, as illustrated in Fig. 2, except that the controlled unit is now the grid of the electron gun (G) rather than the deflection signal generator (D).

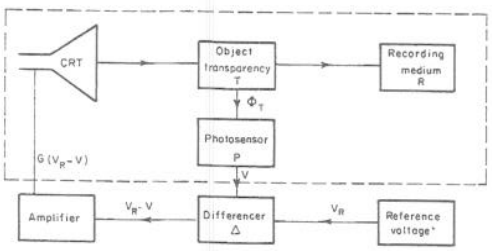

FIG. 3. Closed-loop dynamic exposure control. The total transmitted light, ϕ_T, is sampled by the photosensor and its voltage output, V, is compared to the reference voltage, V_R. The difference is amplified by a factor G and then controls the cathode-ray-tube grid. The upper, boxed portion of the block diagram is identical with the system depicted in Fig. 2 (except for the connection between P and the cathode-ray tube).

The performance of this system is very similar to that of the open-loop system. The exposure at any point x is given by

$$s(x) = c\tau(x)[P \circledast (P \odot \tau + K)^{-1}], \tag{10}$$

where K is the reciprocal of the "loop gain" as defined in the Appendix. The linear version, applicable to low object modulation, leads to a tf:

$$T_p(\nu) = c\left[1 - \frac{|T_s|^2}{1+K}\right]. \tag{11}$$

SUMMARY

A variety of techniques, both linear and nonlinear, are available for restoring the reduction in image spectra at higher spatial frequencies. A number of these have been reviewed here.

APPENDIX: ANALYSIS OF SOME NONLINEAR IMAGE-PROCESSING TECHNIQUES

Here we analyze some of the more complex processing techniques. The analysis is made difficult by the nonlinearity of the processes which also have a finite spread, making them particularly refractory to the usual analytic approaches. When necessary, they are here treated in two steps: a linear finite-spread process followed by a nonlinear zero-spread process.

Each process approaches linearity for low signal levels and this process of "linearization" is carried through for each of them. This enables us to associate a transfer function (tf) with each process, valid whenever the conditions for linearization are met sufficiently closely. A number of the linearized forms here derived have been stated previously [7], but the more important general expressions have not, apparently.

The signal may have the form of luminance, transmittance, reflectance, etc. For the present purposes, the symbol s is used throughout, with subscripts 0, p, etc., designating the original object, the completely processed image, and intermediate stages.

For purposes of linearization, the signal is broken up into two terms: its mean value ($\bar{s}$) and a fluctuating portion ($\tilde{s}$). When the Fourier transform is taken, the constant $\bar{s}$ leads to a delta function at the origin and is tacitly dropped in the following.

Also, the reader is reminded of the normalization assumed for the point-spread function so that the convolution of a spread function with a constant is simply the constant.

1. Photographic Unsharp Masking

In the photographic unsharp masking process, as described in Section 2.1, the print obtainable from a degraded negative is improved by preparing a blurred positive version of the negative, superimposing it on the negative, and printing the two in register.

In general, the photographic process is highly nonlinear and cannot be

represented in a simple analytic form. However, in most emulsions a significant portion of their range can be represented in a form which is linear when density is plotted against the logarithm of exposure. The slope of this line is called gamma and we call its log exposure at zero density log W_0. Note that density is defined as

$$D = -\log \tau, \tag{A1}$$

where τ is the transmittance (or reflectance) of the processed emulsion. Hence the transmittance resulting from an exposure W may be written

$$\tau = (W_0/W)^{\gamma} = kW^{-\gamma}, \; k = W_0^{\gamma}. \tag{A2}$$

We denote the point-spread function of the original recording process by P_1 and that used in preparing the positive mask by P_2. Then an object luminance distribution $s_0(x)$ will result in an image distribution $s_0 \circledast P_1$ and reference to (A2) shows that this, in turn, will yield a negative with transmittance distribution

$$s_1(\mathbf{x}) = k_1 (s_0 \circledast P_1)^{-\gamma_1}. \tag{A3}$$

Similarly, the transmittance of the positive mask will be

$$s_2(\mathbf{x}) = k_2 (s_1 \circledast P_2)^{-\gamma_2}. \tag{A4}$$

When these two transparencies are printed in register, the spread function of the printing process also enters. In practice, however, this can be made negligible and it will, therefore, be neglected here. (If desired, it can be added on as an additional printing process.) Hence, the final image exposure will be simply the product of the two transmittances, and the final image itself will be

$$s_p(\mathbf{x}) = k_p(s_1 s_2)^{-\gamma_p} = k_p \, (k_1^{1-\gamma_2} k_2)^{-\gamma_p} \{(s_0 \circledast P_1)^{-\gamma_1} [(s_0 \circledast P_1)^{-\gamma_1} \circledast P_2]^{-\gamma_2}\}^{\gamma_p}. \tag{A5}$$

This simplifies considerably if

$$\gamma_1 = \gamma_2 = 1/\gamma_p. \text{ Then}$$

$$s_p(\mathbf{x}) = k \, (s_0 \circledast P_1) \, (s_0 \circledast P_1)^{-\gamma_1} \circledast P_2, \tag{A6}$$

where $k = k_p k_1^{1-\gamma_p} k_2^{-\gamma_p}$.

For linearization, we write

$$s_0(\mathbf{x}) = \bar{s}_0 + \tilde{s}_0(\mathbf{x}), \; \tilde{s}_0(\mathbf{x}) \ll \bar{s}_0. \tag{A7}$$

On the assumption of a normalized spread function ($\int P \, dx = 1$), the convolution of P with any constant will equal simply that constant. We can then write the following approximations:

$$s_1 = k_1(\bar{s}_0 + \tilde{s}_0 \circledast P_1)^{-\gamma_1} \approx k_1(\bar{s}_0^{-\gamma_1} - \gamma_1 \bar{s}_0^{-\gamma_1 - 1} \tilde{s}_0 \circledast P_1), \tag{A8}$$

and its spectrum

$$\tilde{S}_1 = -k_1 \gamma_1 \bar{s}_0^{-\gamma_1 - 1} \tilde{S}_0 T_1. \tag{A9}$$

Here we have used subscripted capital S's to indicate the Fourier transform of the signal with the same subscript and a subscripted T to designate the otf (i.e., the Fourier transform of the point-spread function) with the same subscript. Similarly,

$$s_p \approx k_p(k_1k_2)^{-\gamma}\,(s_0^{-\gamma_1}s_1^{-\gamma_2})\left[1+\gamma_p\left(\frac{\gamma_1}{s_0}\,s_0 \bigcirc P_1+\frac{\gamma_2}{s_1}\,s_1 \bigcirc P_2\right)\right], \quad \text{(A10)}$$

and

$$\tilde{S}_2 = -k_2\,\gamma_2 s_1^{-\gamma_1-1}\tilde{S}_1T_2 = k_1k_2\gamma_1\gamma_2\bar{s}_1^{-\gamma_2-1}\tilde{S}_0T_1T_2. \quad \text{(A11)}$$

Again,

$$s_p = k_p\,(s_1s_2)^{-\gamma_p}.$$

On substituting values (A8) and (A10), expanding and dropping all higher-order terms in $\tilde{s}$, we find

$$s_p \approx k_p(k_1k_2)^{-\gamma_p}(\bar{s}_0^{-\gamma_1}\bar{s}_1^{-\gamma_2})\left[1+\gamma_p\left(\frac{\gamma_1}{\bar{s}_0}\,\tilde{s}_0 \circledast P_1+\frac{\gamma_2}{\bar{s}_1}\,\tilde{s}_1 \circledast P_2\right)\right], \quad \text{(A12)}$$

and hence

$$\begin{aligned}\tilde{S}_p &= k\left[\frac{\gamma_1}{\bar{s}_0}\,\tilde{S}_0T_1+\frac{\gamma_2}{\bar{s}_1}\,\tilde{S}_1T_2\right]\\ &= k\,\frac{\gamma_1}{\bar{s}_0}\,\tilde{S}_0T_1\,[1-bT_2],\end{aligned} \quad \text{(A13)}$$

where

$$k = k_p(k_1k_2)^{-\gamma_p}\gamma_p(s_0^{\gamma_1}s_1^{\gamma_2})^{\gamma_p}$$

and

$$b = \frac{\bar{s}_0}{\bar{s}_1}\,\frac{\gamma_2}{\gamma_1}\,k_1\gamma_1\bar{s}_0^{-\gamma_1-1} = \frac{\bar{s}_0^{-\gamma_1}}{\bar{s}_1}\,\gamma_2k_1. \quad \text{(A13.1)}$$

Thus the effective tf of the masking process itself is

$$T_p = T_1(1-bT_2)/(1-b). \quad \text{(A14)}$$

For complete compensation,

$$T_p \sim T_0^{-1}$$

or

$$bT_2 = 1-c/T_0T_1. \quad \text{(A15)}$$

If the positive and negative transparencies are made by independent processes, the linearized approximation to the tf becomes [7]

$$T_p = \gamma_1T_1-\gamma_2T_2. \quad \text{(A16)}$$

2. Fluoro-Dodge

The fluoro-dodge process is, essentially, unsharp masking using phosphor quenching, as described in Section 2.2. Here we analyze its operation, without consideration of the initial and final photographic processes.

The spacing between the transparency and the phosphor causes blurring in two ways:

(1) blurring of the transparency as imaged on the phosphor, and
(2) blurring of the phosphor image on the transparency.

We describe these by the spread functions P_1 and P_2, respectively. These are, in general, not identical.

We also presume that quenching proceeds with a gamma γ_q. Then the luminance distribution on the phosphor will be

$$s_q \sim 1 - a\ (s_1 \circledast P_1)^{\gamma_q}, \tag{A17}$$

and the final photographic exposure will be

$$s_p = (s_q \circledast P_2)s_1 = k_1[s_1 - as_1(s_1 \circledast P_1)^{\gamma_q} \circledast P_2]. \tag{A18}$$

If the quenching process has unity gamma ($\gamma_q = 1$), we can write the spectrum resulting from the fluorododge process immediately:

$$S_p = k_1\ [S_1 - S_1 \circledast (S_1T_1T_2)]. \tag{A19}$$

To enable us to derive an otf for the process, we apply our earlier linearization technique to (A18). This yields

$$s_p = k_1[\bar{s}_1 - a\bar{s}_1^2 + \tilde{s}_1(1 - a\bar{s}_1) - a\bar{s}_1\tilde{s}_1 \circledast P_1 \circledast P_2 - \cdots]. \tag{A20}$$

For the spectrum, this yields

$$\tilde{S}_p = k\ \tilde{S}_1\ [1 - bT_1T_2], \tag{A21}$$

where $b = a\bar{s}_1/(1 - a\bar{s}_1)$.

Thus the otf of the process is [7]

$$T_p = (1 - bT_1T_2)/(1 - b). \tag{A22}$$

3. Masking Using Herschel Effect

Assuming for the Herschel effect a response of the same form as in usual photography:

$$\begin{aligned} s_p(\mathbf{x}) &= k_1[(s_1 \circledast P_1)^{-\gamma_1} - a(s_1 \circledast P_H)^{-\gamma_h}] \\ &= k_1[(\bar{s}_1 + s_1 \circledast P_1)^{-\gamma_1} - a(\bar{s}_1 + s_1 \circledast P_H)^{-\gamma_h} \\ &\approx k_1[\bar{s}_1^{-\gamma_1} - a\bar{s}_1^{-\gamma_H} - \gamma_1\bar{s}_1^{-\gamma_1-1}\tilde{s}_1 \circledast P_1 + a\gamma_H\bar{s}_1^{-\gamma_H-1}\tilde{s}_1 \circledast P_H], \end{aligned} \tag{A23}$$

where γ_H, P_H, and T_H are gamma point-spread function and tf of the Herschel exposure.

Hence,

$$\begin{aligned} S_p &= k_1[-\gamma_1\bar{s}_1^{-\gamma_1-1}\tilde{S}_1T_1 + a\gamma_H\bar{s}_1^{-\gamma_H-1}\tilde{S}_1T_H] \\ &= k[T_1 - bT_H]\tilde{S}_1, \end{aligned} \tag{A24}$$

$$\text{where } k = -\frac{k_1\gamma_1}{\bar{s}^{\gamma_1+1}},\ b = \bar{s}^{\gamma_1-\gamma_H}a\gamma_H/\gamma_1.$$

Thus the tf of the process is [7]

$$T_p = (T_1 - bT_H)/(1-b). \tag{A25}$$

4. Velocity Dynamic Exposure Control

In velocity dynamic exposure control, the scanning spot velocity varies with the total transmitted flux. This flux, in turn, is proportional to the correlation of the spot-spread function P_s and the transmittance τ. Thus the velocity is

$$v = k_0\, s_1 \odot P_s. \tag{A26}$$

The resulting exposure will be the product of the transmittance s_1 and the exposure pattern s_s, generated by the scanning spot. This pattern, in turn, can be seen to be proportional to the convolution of P_s with the reciprocal of the velocity. Thus,

$$s_p = k_1 s_1 s_s = k_1 s_1 \left[\frac{1}{v} \circledast P_s\right] = \frac{k_1 s_1}{k_0}\left[P_s \circledast (s_1 \odot P_s)^{-1}\right]. \tag{A27}$$

For linearization, we find

$$\begin{aligned} s_p &= k_1(\bar{s}_1 + \tilde{s}_1)[k_0^{-1}(\bar{s}_1 + \tilde{s}_1 \odot P_s)^{-1} \circledast P_s] \\ &\approx \frac{k_1}{k_0}(\bar{s}_1 + \tilde{s}_1)[\bar{s}_1 - (\tilde{s}_1 \odot P_s) \circledast P_s \\ &\approx \frac{k_1}{k_0}[\bar{s}_1^2 + \tilde{s}_1\tilde{s}_1 - \bar{s}_1(\tilde{s}_1 \odot P_s) \circledast P_s - \cdots]. \end{aligned} \tag{A28}$$

Note that

$$\mathcal{F}(f \odot g) = \mathcal{F}(f \circledast \hat{g}) = \mathcal{F}(f)\mathcal{F}(\hat{g}) = \mathcal{F}(f)\mathcal{F}^*(g^*),$$

where $\hat{g}(x) \equiv g(-x)$. Noting that P_s is real so that $P_s^* = P_s$, (A28) leads to

$$\tilde{S}_p = \frac{k_1}{k_0}\bar{s}_1[\tilde{S}_1 - \tilde{S}_1 T_s^* T_s] = k\tilde{S}_1[1 - |T_s|^2]. \tag{A29}$$

Thus, the corresponding otf is

$$T_p = 1 - |T_s|^2. \tag{A30}$$

5. Closed-Loop Dynamic Exposure Control (Log Etron)

The reader is referred to Fig. 3 for an illustration of the closed-loop dynamic exposure control system.

The voltage generated by the photosensor is

$$V = \eta\sigma a(\mathbf{x})\ [s \odot P_s], \tag{A31}$$

where η is the fraction of the phosphor radiant flux which is collected onto the photosensor when the object is totally transparent, σ is the photosensor sensitivity in volts/watt or volts/lm, $a(x)$ is the total flux generated in the scanning spot when its center (or other reference point) is at x.

The phosphor flux, in turn, is controlled by the cathode-ray-tube grid voltage, which is the amplified difference between V and the reference voltage V_R:

$$a = g\,G\,(\mathrm{V}_R - \mathrm{V}), \tag{A32}$$

where g is the cathode-ray-tube phosphor flux per unit grid voltage (W/V or lm/V), and G is the gain of the voltage amplifier.

Eliminating V between (A31) and (A32) and solving for a, we find

$$a = k[s \odot P_s + K]^{-1}, \tag{A33}$$

where $k = \mathrm{V}_R/\eta\sigma$, and $K = 1/\eta\sigma g G$ is the reciprocal of the loop gain.

Thus, during the scanning of a full raster, an integrated luminance distribution will be generated of the form $a \circledast P_s$. This must be multiplied by the transmittance, s, to yield the net exposure, which is

$$W(\mathbf{x}) = s \cdot a \bigcirc P_s = ks\left(\frac{1}{s \odot P_s + K}\right) \circledast P_s. \tag{A34}$$

This expression permits the calculation of the exposure resulting from any object transparency s (x).

For linearization, we again follow the approach used earlier in this Appendix:

$$W(\mathbf{x}) = k(\bar{s} + \tilde{s})\left[\frac{1}{\bar{s} + \tilde{s} \odot P_s + K} \circledast P_s\right].$$

On expanding and dropping terms of higher order in $\tilde{s}$, we find

$$W(\mathbf{x}) \approx \frac{k}{\bar{s} + K}\,\bar{s} - \frac{\bar{s}}{\bar{s} + K}\,\tilde{s} \odot P_s \circledast P_s + \tilde{s},$$

and, hence,

$$S_p = \frac{k}{\bar{s} + K}\,S_1\left(1 - \frac{|T_s|^2}{\bar{s} + K}\right),$$

and the equivalent tf is

$$T_p = 1 - |T_s|^2/(\bar{s} + K).$$

REFERENCES

1. G. SPIEGLER AND K. JURIS, Ein neues Verfahren zur Herstellung ausgeglichener Kopien nach besonders harten Originalaufnahmen, *Phot. Korr.* **67**, 1931, 4–9, see also **69**, 1933, 36–41.
2. J. A. C. YULE, Unsharp masks and a new method of increasing definition in prints, *Phot. J.* **84B**, 1944, 321–327.
3. G. SPIEGLER AND K. JURIS, Ein neues Kopierverfahren zur Herstellung ideal harmonischer Kopien nach kontrastreichen Negativen, *Fortschritte Roentgenstrahlen* **42**, 1930, 509–518.
4. J. A. EDEN, The unsharp mask technique of printing aerial negatives, *Photogram. Record* **1**, 1955, 5–26.
5. J. ST. CLAIR AND M. MERRIAM, The use of photography to achieve basic principles of map design, *Photogram. Eng.* **26**, 1960, 498–504.

6. J. D. ARMITAGE, A. W. LOHMANN, AND R. B. HERRICK, Absolute contrast enhancement, *Appl. Opt.* **4**, 1965, 445–451.
7. A. LOHMANN, Aktive Kontrastübertragungstheorie, *Opt. Acta* **6**, 1959, 319–338.
8. *Line Effects from Photographs by the Kodak Tone-Line Process*, Eastman-Kodak Co., Rochester, 1966. This is Kodak Pamphlet No. Q-18.
9. D. CURIE, *Luminescence in Crystals*, p. 199, Methuen, London, 1963.
10. C. E. K. MEES AND T. H. JAMES, *The Theory of the Photographic Process*, 3rd ed., pp. 155–160, Macmillan, New York, 1966.
11. M. JOHNSON, Use of the Herschel effect in improving aerial photographs, *J. Opt. Soc. Amer.* **41**, 1951, 748–751.
12. D. H. KELLY, Image-processing experiments, *J. Opt. Soc. Amer.* **51**, 1961, 1095–1101.
13. A. J. WATSON, The fluoro-dodge method for contrast control, *Photogram. Eng.* **24**, 1958, 638–643.
14. A. B. CLARKE, A photographic edge isolation technique, *Photogram. Eng.* **28**, 1962, 393–399.
15. P. DUMONTET, Machine élaborant des produits de composition en vue de la correction de certain defauts dus à la diffraction, *Opt. Acta* **3**, 1956, 145–146.
16. A. J. HANNUM, Techniques for electronic image enhancement, Soc. Photogr. Instr. Eng., *Proc. SPIE Image Enhancement Seminar*, March 1963.
17. R. V. SHACK, Image processing by an optical analog device, *Pattern Recogn.* **2**, 1970 123–126.
18. L. SWINDELL, A noncoherent optical analog image processor, *Appl. Opt.* **9**, 1970, 2459–2469.
19. S. W. LEVINE AND H. MATE, Selected electronic techniques for image enhancement, Soc. Photogr. Instr. Eng., *Proc. SPIE Image Enhancement Seminar*, March, 1963, Part II.
20. W. F. SCHREIBER, Wirephoto quality improvement by unsharp masking, *Pattern Recogn.* **2**, 1970, 117–121.
21. P. PARGAS, The principle of velocity modulation dodging, *Phot. Sci. Eng.* **9**, 1965, 219–227.
22. D. R. CRAIG, The log etron: A fully automatic servo-controlled scanning light source for printing, *Phot. Eng.* **5**, 1954, 219–226.